International Journal of Advanced Science and Technology
Vol.69 (2014), pp.19-32
http://dx.doi.org/10.14257/ijast.2014.69.03

Performance Evaluation of Optic Disc Segmentation Algorithms in Retinal Fundus Images: an Empirical Investigation

Medha V. Wyawahare[1] and Dr. Pradeep M. Patil[2]

[1]*Vishwakarma Institute of Technology, Bibwewadi, Pune, India*
[2]*RMD Sinhgad Technical Institutes' Campus, Warje, Pune, India*

Abstract

Careful evaluation of Optic nerve head structure and its documentation is extremely important for diagnosis of Glaucoma, an eye disease which leads to vision loss. This work focuses on automatic segmentation of Optic disc from fundus images, which is an important parameter for disease diagnosis. We investigate and compare performance of five methods used for Optic disc segmentation. These five methods are based on use of algorithms namely; distance regularized level set, Otsu thresholding, region growing, particle Swarm optimization, generalized regression neural network. For ease of comparison all the methods were implemented and tested on a single database. The method using generalized regression neural network best suits the said application. It outperforms the other four due to highest region agreement, lowest non overlap ratio, lowest relative absolute area difference and low execution time.

Key words*: Optic nerve head, optic disc, fundus image*

1. Introduction

Glaucoma is progressive degeneration of the retinal ganglion cells and optic nerve axons. Left untreated, it causes irreversible damage to the optic nerve and retinal fibers resulting in a progressive, permanent loss of vision. Visual Field loss is the late manifestation of the disease. In Glaucoma, detectable structural changes in the optic nerve head (ONH) precede detectable functional changes in the visual field. Hence diagnosis of Glaucoma at an early stage is vital. Early treatment reduces rate of progression of the disease thus preventing visual field loss and blindness. Comprehensive examination of the patient's ONH helps in early Glaucoma diagnosis [1, 2]. The ONH structure comprises of the optic disc (OD) and the optic cup (OC). The cup to disc ratio is one of the vital parameters used for Glaucoma diagnosis. A Computer aided diagnostic (CAD) system can assist the ophthalmologists in computing this ratio. To compute this ratio the OD and OC need to be segmented and quantified. This work focuses on automatic segmentation of OD from ONH structure. Automation is intended to eliminate the inter-operator variability in segmentation and removing subjectivity in the decision. A number of methods have been implemented in this respect which is reviewed in section 1.1. Efficient algorithms for localization and segmentation of OD are difficult to achieve due to variable appearance and occlusion due to optic nerves [3]. Secondly, a robust segmentation algorithm which would give correct segmentation results over a large database also seems to be difficult to achieve. The aim of the present work is to compare the performance of various segmentation methods in the context of said application.

ISSN: 2005-4238 IJAST

2. Review of OD Segmentation Methods

Walter and Klein [3] have localized optic disc by binary thresholding in HLS color space and then used watershed transform to find the exact contours. James Lowell, *et al.,* [4] have achieved optic disk localization using specialized template matching and segmentation by a deformable contour model. Inoue, *et al.,* [5] used average, variance, standard deviation of all pixels for calculating threshold while segmenting the optic disc. To detect the initial contour of the optic disc Jlassi Hajer, *et al.,* [6] have used the watershed transform and finally the optic disk boundary was determined using active contours called watersnake. S.Sekhar [7] first isolated the brightest area in the image by means of morphological processing, and then used Hough transform to detect optical disk. Jagadish Nayak, *et al.,* [8] have performed morphological operations on red channel followed by threshoding to segment optic disc. The threshold value is decided by the standard deviation. To localize the optic disc D. W. K. Wong, *et al.,* [9] have obtained histogram of the fundus image 0.5% of all pixels in the grayscale fundus image with the highest intensity are selected as the disc region has higher intensity. A circle with a radius of twice the typical normal optic disc radius value and centered at the disc center is used to determine the ROI, with the circle used as the initial contour for segmentation using variational level-set approach. Aquino A., *et al.,* [10] used morphological techniques and edge detection techniques followed by hough transform for circular approximation of optic disc boundary. Joshi, *et al.,* [11] used deformable model guided by regional statistics to detect optic disc boundary. Kavitha, *et al.,* [12] used manual threshold analysis, color component analysis and region of interest based segmentation for optic cup extraction. Fengshou Yin, *et al.,* [13] have used edge detection and the Hough Transform combined with a statistical deformable model to extract the OD boundary. Jun Cheng, *et al.,* [14] proposed an optic disc segmentation method based on superpixel classification. In the classification, histograms from contrast enhanced image channels and center surround statistics from center surround difference maps are used as features to determine each superpixel as disc or non disc. Shys-Fan Yang-Mao, *et al.,* [15] proposed to choose the ROI using statistical features including the mean, standard deviation, and skewness of the pixel gray-levels in the candidate regions from a set of candidate rectangular regions. Maximal inscribed circle is treated as the initial contour of the optic disc. This method uses an active contour model (ACM) to precisely segment the optic disc further based on the initial contour. Ellipse fitting is often used to smoothen the OD contour, once detected [9, 13, 14]. Chisako Muramatsu, *et al.,* [16] have compared active contour model method with Fuzzy X means clustering and artificial neural network (Back propogation algorithm) methods used for OD segmentation.

3. Image Database

A public database, DRIONS_DB has been used for benchmarking optic nerve head segmentation [17]. As reported by [17] the database consists of 110 colour digital retinal images, collected at Ophthalmology Service at Miguel Servet Hospital, Saragossa (Spain). The average age of the patients was reported as 53 years (S.D. 13.05) (46.2% male and 53.8% female). 23.1% patients had chronic simple glaucoma and 76.9% eye hypertension. The images were acquired with a colour analogical fundus camera. In order to have the images in digital format, they were digitized using a HP-PhotoSmart-S20 high-resolution scanner and stored in RGB format with resolution 600x400 (8 bits/pixel). For cross validating the results of segmentation algorithms, [17] provides independent contours from two medical experts. These were collected by using a software tool provided for image annotation. An inter-observer variability is observed among the two experts tracing the contour. The average of the

two was considered as ground truth in the current work. The database was divided into two paradigms, the training and the testing dataset. 45 randomly selected images were used for training while the remaining 65 were used for testing purpose.

3. Methodology

Figure 1 shows the steps carried out in segmenting the OD which is explained below sequentially.

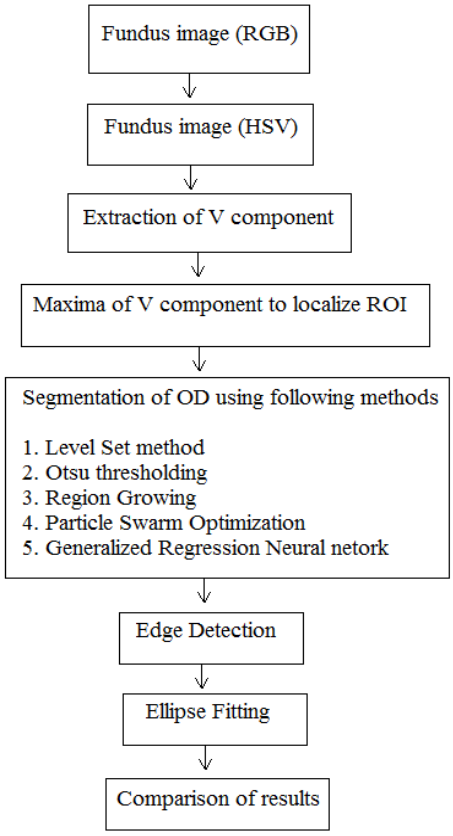

Figure 1. Steps in the Segmentation Process

HSV Color Space

The RGB fundus image was converted to HSV color space since its V component of was found to highlight the OD region and was further used for processing. HSV color space is formulated by looking at the RGB color cube along its gray axis which results in hexagonal shape color pallete [18]. Along the vertical (gray) axis the size of hexagonal plane that is perpendicular to the axis changes. Hue is an angle around a color hexagon. The 0^0 axis is red axis. Value is measured along the axis of the cone. The V=0 end of the axis is black and V=1 end of the axis is white. It lies at the center of the color hexagon. Thus the axis represents all shades of gray. Saturation (purity of color) is measured as a distance from V axis. The model created by A. R. Smith is closer to human experience and color sensations than RGB system. Hue, saturation and value refer approximately to tint shade and tone. Converting RGB to HSV is a matter of converting Cartesian coordinates to cylindrical coordinates.

Localization of OD

OD is seen as the brightest portion in the V component of the HSV image. Hence centroid of the optic disc is calculated as the mean of coordinates of pixels with maximum intensity. The image is cropped as a 200 x 200 matrix taking centroid as centre. Thus the region of interest is extracted.

Segmentation of OD

The cropped image extracted from the v component is subjected for further segmentation for extracting the OD region. Five alternative methods were implemented for OD segmentation, with a sole aim to compare their performance in the context of the said application. The five alternative methods are distance regularized level set evolution, otsu thresholding, region growing, particle Swarm optimization, generalized regression neural network. The methods are explained in Sections 3.1 to 3.5.

3.1. Distance Regularized Level Set Evolution Method

Chunming Li, *et al.*, [19] have proposed a new type of level set evolution called Distance regularized Level Set evolution method (DRLSE) and its application to image segmentation. [19] Proposed application of DRLSE to an edge-based active contour model for image segmentation. The active contour model in DRLSE formulation allows the use of relatively large time steps to significantly reduce iteration numbers and computation time.
Let Φ be a LSF defined on a domain Ω. We define energy functional by

$$E(\Phi) = \mu Rp(\Phi) + Eext(\Phi)$$

The level set regularization term is defined by

$$p(\Phi) = \int_{\Omega} p(|\nabla|)dx$$

where p is potential or energy density function. Simple definition of potential p for distance regularization is

$$p = p_1(s) \triangleq \frac{1}{2}(s-1)^2$$

which has $s=1$ as unique minimum point. With this potential $p=p_1(s)$ the level set regularization term $Rp(\Phi)$ can be expressed as

$$\frac{\partial \Phi}{\partial t} = (|\nabla \Phi|) - 1)^2 dx$$

The gradient flow of energy $E(\Phi)$ is $\frac{\partial \Phi}{\partial t} = \mu div(dp(\nabla \Phi)\nabla \Phi) - \frac{\partial E_{ext}}{\partial \Phi}$
The distance regularization effect of DRLSE can been seen from the gradient flow of energy $\mu Rp(\Phi)$.

$$\frac{\partial \Phi}{\partial t} = \mu div(dp(\nabla \Phi)\nabla \Phi)$$

Following equation is an edge-based geometric active contour model, which is an application of the general DRLSE formulation in image segmentation.

$$\frac{\partial \Phi}{\partial t} = \mu div(dp(|\nabla \Phi|)\nabla \Phi) + \lambda \delta_E(\Phi) div\left(g \frac{\nabla \Phi}{|\nabla \Phi|}\right) + \alpha g \delta_E(\Phi)$$

where g is the edge indicator function, μ is the weight of distance regularization term, λ is the weight of the weighted length term, α is the weight of the weighted area term. We experimented with different parameter settings. Parameters chosen for best results are α = -10, λ = 5, μ = 0.1.

3.2. Otsu Thresholding

Otsu's method selects the threshold by minimizing the within-class variance of the two groups of pixels separated by the thresholding operator [20]. Consider that we have an image with L gray levels and its normalized histogram. For each gray-level value i, $P(i)$ is the normalized frequency of i. Assuming that we have set the threshold at T, the normalized fraction of pixels that will be classified as background and object will be

$$q_b(T) = \sum_{i=1}^{T} P(i) \text{ and}$$

$$q_0(T) = \sum_{i=T+1}^{L} P(i)$$

The variance of the background and the object pixels will be

$${\sigma_b}^2(T) = \frac{\sum_{i=1}^{T}(i-\mu_b)^2 \ P(i)}{\sum_{i=1}^{T} P(i)} = \frac{1}{q_b(T)} \sum_{i=1}^{T} (i-\mu_b)^2 \, P(i)$$

$${\sigma_0}^2(T) = \frac{\sum_{i=T+1}^{L}(i-\mu_0)^2 \ P(i)}{\sum_{i=T+1}^{L} P(i)} = \frac{1}{q_0(T)} \sum_{i=T+1}^{L} (i-\mu_0)^2 \, P(i)$$

Where $\mu_b \ and \ \mu_0$ represent mean gray level values of background and object pixels respectively. The variance of the whole image is

$$\sigma^2 = \sum_{i=1}^{L} (i-\mu)^2 \, P(i)$$

Where μ represents mean gray level value of entire image. Variance can be written as follows

$$\sigma^2 = q_b(T){\sigma_b}^2(T) + q_0(T){\sigma_0}^2(T) + q_b(T)(\mu_b(T)-\mu)^2 + q_0(T)(\mu_0(T)-\mu)^2$$
$$= {\sigma_W}^2(T) + {\sigma_B}^2(T)$$

Where ${\sigma_W}^2(T)$ is the within-class variance and ${\sigma_B}^2(T)$ is the between-class variance. Since the total variance does not depend on T, the T minimizing ${\sigma_W}^2(T)$ will be the T maximizing ${\sigma_B}^2(T)$. Let's consider maximizing ${\sigma_B}^2(T)$, we can rewrite ${\sigma_B}^2(T)$ as

$${\sigma_B}^2 = \frac{(\mu(T) - \mu q_B(T))^2}{q_B(T) q_0(T)}$$

where $\mu(T) = \sum_{i=1}^{T} i \, P(i)$.

We start from the beginning of the histogram and test each gray-level value for the possibility of being the threshold T that maximizes ${\sigma_B}^2(T)$. Once T is determined using the image is converted to binary using thresholding. The binarization process segments the OD region which is subsequently subjected to edge detection.

3.3. Region Growing

Region growing is a procedure that group's pixels or sub-regions into larger regions based on predefined criteria. The basic approach is to start with a set of "seed" points and from these grow regions by appending to each seed those neighboring pixels that have properties similar to the seed (such as specific ranges of gray level or color) [18].

Let R be the entire region partitioned into n subregions, R1, R2, …, Rn such that

$$\bigcup_{i=1}^{n} R_i = R$$

R_i is a connected region i=1,2,...,n

$$R_i \cap R_j = \emptyset \; for \; i \neq j$$
$$P(Ri) = \; true \quad \forall$$
$$P(Ri \cup Rj) = \; false$$
$$for \; any \; adjacent \; Ri \; and \; Rj$$

*P(Rk)*is a logical predicate defined over the points in *Rk*.

We group pixels or subregions into larger regions based on predefined criteria. We start with a seed point and from this grow OD region by appending to each seed those neighboring pixels that have properties similar to the seed. The threshold value selected to test whether a pixel is sufficiently similar to other pixel is 0.2.

3.4. Particle Swarm Optimization

Particle Swarm Optimization (PSO) is a computational method which tries to find optimum solution iteratively by improving the candidates solution with the known measure of quality. The candidates solution is called as 'particle'. The rate of position change is called as 'velocity'. 'Fitness' is the measure of quality. The PSO method is described below [21]. Each particle is treated as a point in an *n*-dimensional space. The *i*th particle is represented as$x_i = (x_{i1}, x_{i2}, \dots x_{in})$. The best previous position *pbest* of the *i*th particle is recorded and represented as $p_i = (p_{i1}, p_{i2}, \dots p_{in})$. the index of the best particle among all the particles in the population (global model) is represented by the subscript *g*. The index of the best particle among all the particles in a defined topological neighborhood (local model) is represented by the subscript *l*. The rate of the position change (velocity) for particle *i* is represented by $v_i = (v_{i1}, v_{i2}, \dots v_{in})$. The particles are manipulated according to the following equations (global model)

$$v_{id} = w_i * v_{id} + c_1 * rand( ) * (p_{id} - x_{id}) * Rand( ) * (p_{gd} - x_{id})$$

$$x_{id} = x_{id} + v_{id}$$

where *d* is the dimension ($1 \leq d \leq n$), c_1 and c_2 are positive constants, *rand( )* and *Rand( )* are two random functions in the range [0,1], and *w* is the inertia weight. For the global model, above equation is used to calculate a particle's new velocity according to its previous velocity and the distances of its current position from its own best experience (pbest) and the group's best experience (gbest). The performance of each particle is measured according to a predefined fitness function, which is related to the problem to be solved. The inertia weight *w* controls the impact of the previous histories of velocities on the current velocity. It was chosen to be 1.2. Individual and social weight of particle was 0.8. One of the issues while implementing PSO method was initializing the population size. It was randomly initiated to 150. The positions and velocities of particles were also randomly selected. The algorithm

performed 150 iterations.

3.5. Generalized Regression Neural Network

The OD region can be segmented by converting the image to binary by single thresholding. A V component image is turned into a binary image by choosing a V level *T* in the original image, and then turning every pixel black or white according to whether its V value is greater than or less than *T*. However, use of manual thresholding doesn't automate the process. Also selecting threshold within a certain range fails to work on a database with wide variety of images. A need of estimator was felt to estimate threshold value for every individual image. This was done using generalized regression neural network (GRNN). GRNN was trained to predict threshold value for every image in the database. Input to GRNN was a set of statistical features like minima, maxima, standard deviation, median, kurtosis computed from gray level histogram of V component of the image. The network output is the threshold value required for segmentation of OD. The OD is segmented by binary thresholding using the threshold predicted by GRNN. Many more features could have been used but that would increase the network complexity. Also the feature set selected was found to be most useful in predicting the threshold. Generalized regression neural networks are a kind of radial basis network that is often used for function approximation. The input units are distribution units. They provide measurement variables $\boldsymbol{X}$ to the neurons in the second layer, which are the pattern units. The pattern unit belongs to one cluster center. When a new vector $\boldsymbol{X}$ is entering the network, is subtracted from the stored vector which belongs to cluster center. Squares or the absolute values of the differences are added up and passed to a nonlinear activation function. The activation function used is exponential. The pattern unit outputs are given to the summation units. A dot product of a weight vector and a vector composed of the signals from the pattern units is carried out at the summation unit. The summation unit sums the outputs of the pattern units weighted by the number of observations of every cluster center. It gives the estimate of $\boldsymbol{f(X)K}$. Constant $\boldsymbol{K}$ is determined by the Parzen window. The summation unit multiplies each value from a pattern unit by the sum of samples $\boldsymbol{Y}^j$ for cluster center $\boldsymbol{X}^{i.}$ It estimates $\hat{\boldsymbol{Y}}\boldsymbol{f(X)K}$. Division is carried out at the output unit. $\hat{\boldsymbol{Y}}\boldsymbol{f(X)K}$ is divided by $\boldsymbol{f(X)K}$. It gives the estimate of $\boldsymbol{Y}$. An extra summation unit is used for estimation of each component. Sums of samples of the component of $\boldsymbol{Y}$ for each cluster center $\boldsymbol{X}^i$ are used as multipliers. The output vector requires only one summation neuron and one output neuron. All the neurons can operate in parallel since they are not interactive. A microprocessor assigns training patterns to cluster centers and updates the coefficients $\boldsymbol{A}^i$ and $\boldsymbol{B}^{i.}$. K-means averaging can also be used for updating cluster centers. The network can be trained in iteration with the training data.

$$\hat{\mathrm{Y}}(X) = \frac{\sum_{i=1}^{n} Y^i \exp(-\frac{C_i}{\delta})}{\sum_{i=1}^{n} \exp(-\frac{C_i}{\delta})}$$

$$C_{i=} \sum_{i=1}^{n} |X_i - X_j|$$

The coefficients are determined in one iteration; no iterative algorithm is required. The training data was sufficient due to the quick learning and fast convergence by GRNN. The performance of threshold prediction by GRNN was obtained by cross correlation of actual and predicted threshold values. Figure 2 shows the GRNN architecture and the correlation of actual and predicted threshold values.

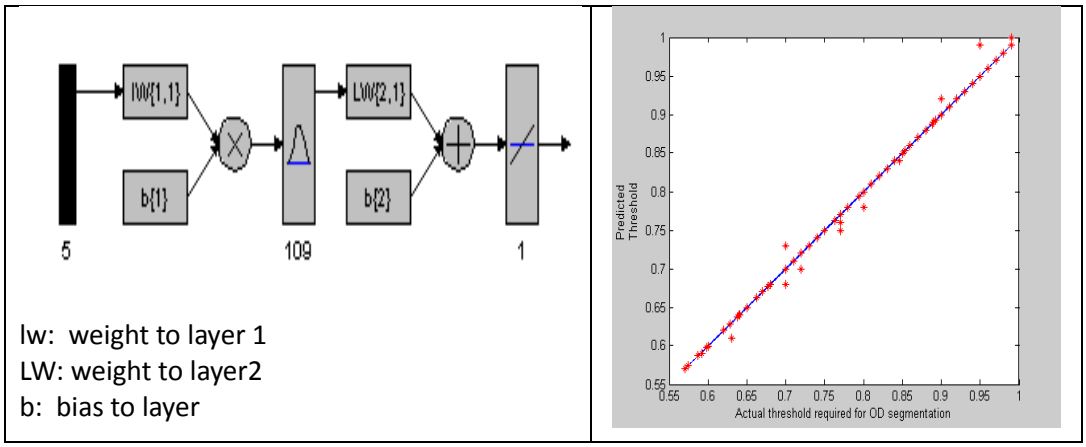

Figure 2. GRNN Architecture and Correlation of Required and Predicted Threshold Values

4. Edge Detection

After segmenting the OD region, the boundary of the OD is detected using Canny Edge Detection technique. This method finds edges by looking for local maxima of the gradient of the image. The gradient is calculated using the derivative of a Gaussian filter. The method uses two thresholds, to detect strong and weak edges, and includes the weak edges in the output only if they are connected to strong edges. This method is therefore more immune to noise. Canny edge detector follows the following steps [23].

1. Elimination of noise by smoothing of the image.
2. Finding gradient to mark regions with high magnitude gradients.
3. Amongst the marked regions it suppresses the non maximum pixels.
4. Double thresholding is done with hysteresis. If the magnitude is above the high threshold, it is marked as an edge. The OD contour is smoothened using ellipse fitting algorithm.

5. Results

The performance of the five methods was evaluated using following parameters. If A is the disc area provided by the ground truth and B is the disc area calculated using the method under test, then

1. $Region\ agreement$ [16]

RA= $\frac{A \cap B}{A \cup B}$ (Ideally 1)

2. $Non\ overlap\ ratio$ [24]

NOR= $1 - \frac{A \cap B}{A \cup B}$ (Ideally 0)

3. $Relative\ absolute\ area\ difference$ [24]

$RAD = \frac{abs(A-B)}{A}$ (Ideally 0)

4. $Execution\ time\ (in\ \text{sec})$

Table 1 shows the performance metrics calculated for all the five methods under test. They are the average values calculated in the dataset of 110 images.

Table 1. Comparison of Different Segmentation Methods based on Performance Parameters

Method	Region Agreement	Non overlap ratio	Relative absolute area difference	Execution time (sec)
Level Set	0.67185	0.324815	0.66256	2.984038
Otsu thresholding	0.735895	0.254845	0.459806	0.514154
Region growing	0.752469	0.247531	0.179534	0.448121
Particle swarm optimization	0.80555	0.19445	0.224228	22.69907
GRNN	0.839094	0.160906	0.121526	0.473661

Figure 3 demonstrates graphically comparison of different methods based on performance parameters. Figure 4 shows the OD extracted in sample fundus images by different methods. It can be seen that GRNN method outperforms the other four due to highest region agreement, lowest non overlap ratio, lowest relative absolute area difference and low execution time. Despite less execution time Otsu thresholding and region growing methods suffer from the drawback of low region agreement. PSO method has a better region agreement but poor execution time. Level set method exhibits lowest region agreement, largest relative absolute area difference and comparatively larger execution time.

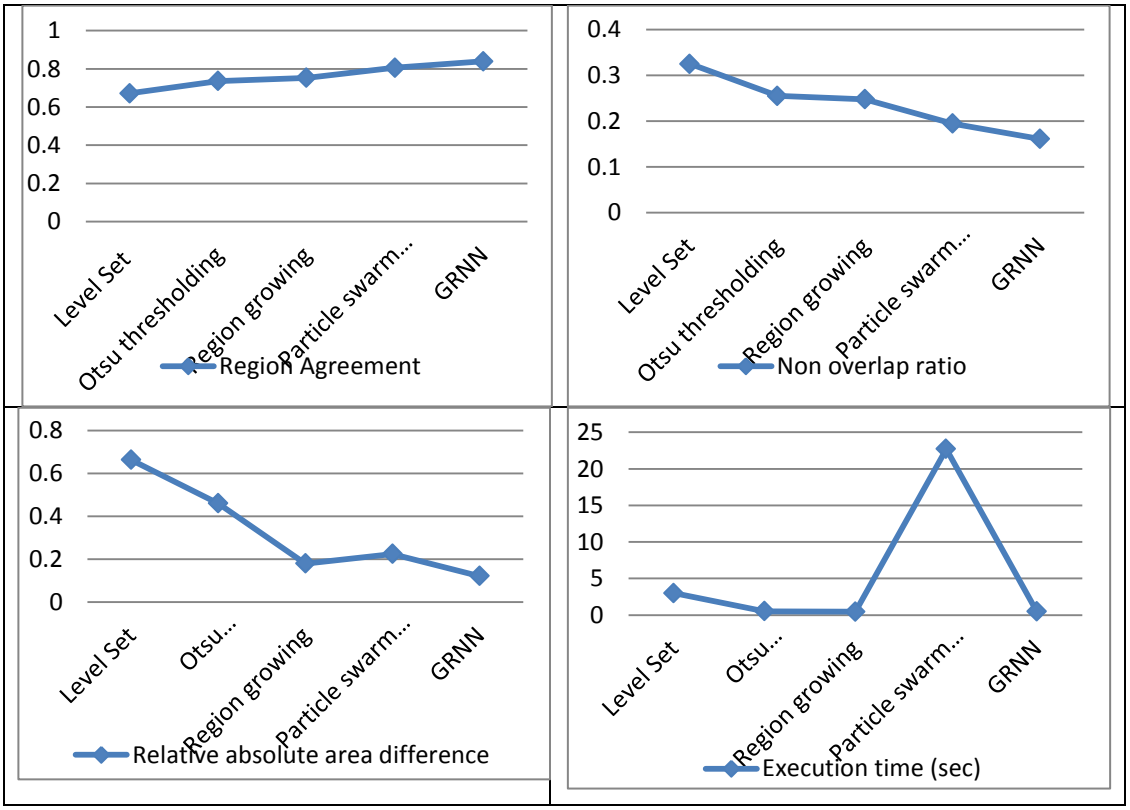

Figure 3. Graphs Demonstrating Comparison of Performance of Different Methods

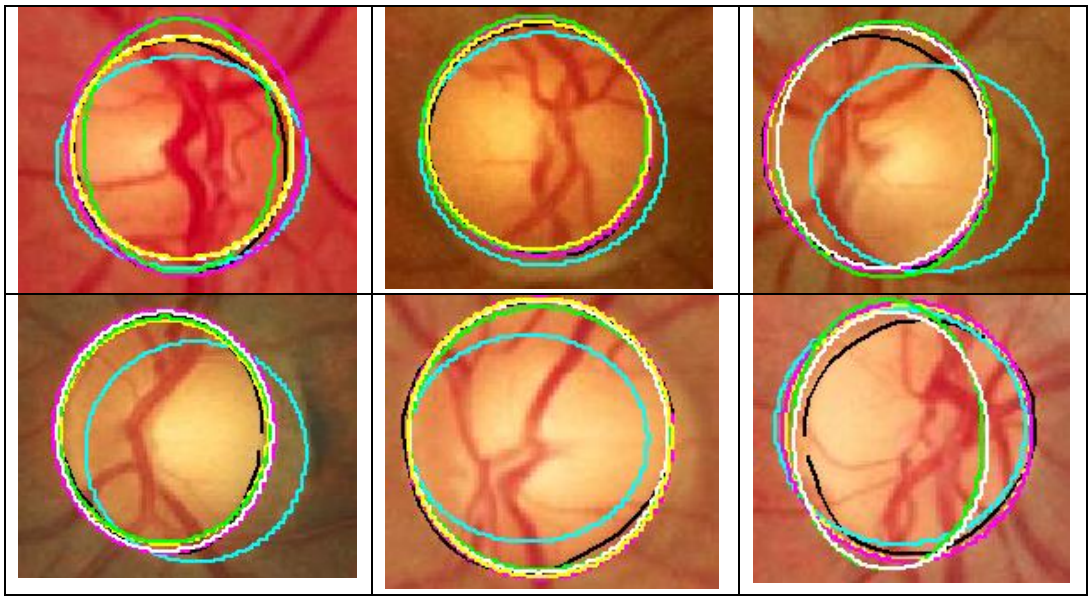

Figure 4. Segmented OD in Sample Images. Cyan, Magenta, Green, White and Yellow Coloured Boundaries Represent OD Segmentation by DRLSE, Otsu Thresholding, Region Growing, Particle Swarm Optimization, Generalized Regression Neural Network Methods Respectively

5. Discussion

Implementing a computer assisted diagnostic system for disease diagnosis has been always a desirable area for researchers and many attempts are seen in this direction [25-27]. Detection and quantification of optic Disc is one of the crucial factors in diagnosis of Glaucoma, an eye disease. The aim of the research was to investigate the suitability of segmentation methods in OD extraction. We have reported an empirical comparison of five different segmentation methods in context of the said application. Performance of the five different segmentation methods was evaluated in terms of segmentation accuracy and disparity from clinical values. The performance metrics used gave a fair reflection of these aspects. We believe that use of open access database with ground truth is a desirable feature since the work can be further compared with the results of other research groups. The entire dataset was divided into two paradigms for training and testing purpose. Training dataset comprised of 45 images whereas the testing dataset comprised of 65 images. Choice of HSV model over RGB was done in order to highlight the OD region which was very prominent in V component. The V component was subjected to further segmentation steps. Extraction of ROI with OD as the centre proved to be effective in eliminating false segmentation. While implementing DRLSE method, we experimented with different parameter settings and best results were obtained with $\alpha = -10$, $\lambda = 5$, $\mu = 0.1$. An important feature of DRSE method is it allows efficient initialization of parameters. One of the issues while implementing PSO method was initializing the population size. It was randomly initiated to 150. The positions and velocities of particles were also randomly selected. More research in this aspect may be done to fine tune these parameters and reduce the computational cost involved. While implementing GRNN method feature set selected intuitively comprising of minima, maxima, standard deviation, median and kurtosis made the classification work extremely well. But a more organized approach of selecting features optimally out of a larger feature set by making use of statistical feature selection methods may also be explored. Region agreement which

depicts the accuracy of segmentation was found to improve sequentially in Level set, Otsu thresholding, region growing, particle swarm optimization and GRNN methods. Results show that out of the five implemented methods the GRNN based method has proved to be more accurate and computationally efficient with region agreement of 0.839, non overlap ratio of 0.16, relative absolute area difference of 0.12 and execution time of 0.473. Particle swarm optimization method performs fairly well with region agreement of 0.80, non overlap ratio of 0.19 and relative absolute area difference of 0.22 but suffers from a drawback of high computational time.

6. Conclusion

Careful evaluation of ONH structure and its documentation is extremely important for diagnosis and monitoring of Glaucoma. We focused on automatic segmentation of Optic disc from fundus images, which is an important parameter for the disease diagnosis. We investigated and compared performance of five methods namely; distance regularized level set, Otsu thresholding, region growing, particle swarm optimization, generalized regression neural network used for Optic disc segmentation. For ease of comparison all the methods were implemented and tested on a single database. The method using generalized regression neural network best suits the said application. It outperforms the other four due to highest region agreement, lowest non overlap ratio, lowest relative absolute area difference and low execution time.

Acknowledgements

The authors are thankful to the Carmona E.J., Rincon M., Feijoo J.G., Martinez-de-la-Casa J.M. for making the public database DRIONS_DB and the ground truth available. We acknowledge the help of Dr. Medha Prabhudesai and Dr. Mandar Paranjpe, Ophthalmologists for their guidance in understanding glaucoma and its diagnosis procedure. We also acknowledge the help of Dr. Mandar Paranjpe in validation of results.

References

[1] Dr. M. Prabhudesai, "Atlas of Optic Nerve Head Evaluation in Glaucoma", New Delhi, Jaypee Brothers Medical Publishers (P) Ltd., **(2006)**.
[2] M. Fingeret, F. A. Medeiros, R. Susanna and R. N. Weinreb, "Five rules to evaluate the optic disc and retinal nerve fiber layer for glaucoma", Optometry, vol. 76, **(2005)**, pp. 661-668.
[3] T. Walter and J. C. Klein, "Segmentation of color fundus images of human retina: detection of the optic disc and the vascular tree using morphological techniques", ISMDA 2001, LNCS, vol. 2199, **(2001)**, pp. 282–287.
[4] J. Lowell, A. Hunter, D. Steel, A. Basu, R. Ryder, E. Fletcher and L. Kennedy, "Optic nerve head segmentation", IEEE transactions on medical imaging, vol. 23, **(2004)**, pp. 256-264.
[5] N. Inoue, K. Yanashima, K. Magatani and T. Kurihara, "Development of a simple diagnostic method for the glaucoma using ocular Fundus pictures", Conference Proceedings of IEEE Engineering in Medicine and Biology, **(2005)**, pp. 3355-3358.
[6] J. Hajer, H. Kamel and E. Noureddine, "Localization of the optic disk in retinal image using the water snake", Proceedings of International conference on Computer and Communication Engineering, **(2008)**, pp. 947-951.
[7] S. Sekhar, W. Al-Nuaimy and A. K. Nandi, "Automated localization of retinal optic disk using hough transform", 5th IEEE International Symposium on Biomedical Imaging: From Nano to Macro, **(2008)**, pp. 1577-1580.
[8] J. Nayak, R. Acharya, P. S. Bhat, N. Shetty and T. C. Lim, "Automated Diagnosis of Glaucoma Using Digital Fundus Images", Journal of Medical Systems, vol. 33, **(2009)**, pp. 337-346.
[9] D. W. K. Wong, J. Liu, J. H. Lim, X. Jia, F. Yin, H. Li and T. Y. Wong, "Level set based automatic cup-to-disc ratio determination using retinal fundus images in Argali", Proceedings of 30th Annual International IEEE EMBS Conference Vancouver, British Columbia, Canada, **(2008)**, pp. 2266-2269.

[10] A. Aquino, M. E. Gegundez-Arias and D. Marin, "Detecting the optic disc boundary in digital fundus images using morphological, edge detection, and feature extraction techniques", IEEE Trans Med Imaging, vol. 29, **(2010)**, pp. 1860-1869.
[11] G. D. Joshi, J. Sivaswami, K. Karan and S. R. Krishnadas, "Optic Disk and cup boundary detection using regional information", IEEE International Symposium on Biomedical Imaging: From Nano to Macro, **(2010)**, pp. 948- 951.
[12] S. Kavitha, S. Karthikeyan and Dr. K. Duraiswami, "Neuro retinal rim quantification in fundus images to detect glaucoma", International journal of computer science and network security, vol. 10, **(2010)**, pp. 134-140.
[13] F. Yin, J. Liu, D. W. K. Wong, N. M. Tan, C. Cheung, M. Baskaran, T. Aung and T. Y. Wong, "Automated Segmentation of Optic Disc and Optic Cup in Fundus Images for Glaucoma Diagnosis", 25th International Symposium on Computer-Based Medical Systems (CBMS), **(2012)**, pp. 1-6.
[14] J. Cheng, J. Liu, Y. Xu, F. Yin, D. W. K. Wong, N. M. Tan, C. Y. Cheng, Y. C. Tham and T. Y. Wong, "Superpixel Classification based Optic Disc Segmentation", Proceedings of the 11th Asian conference on Computer Vision - Volume Part II , **(2010)**, pp. 293-304.
[15] S. F. Y. Mao, Y. F. Chen, C. M. Wang, Y. K. Chan and Y. P. Chu, "A statistics-based initial contour detection of optic disc on a retinal fundus Image Using Active Contour Model", Journal of medical and biological engineering, vol. 33, **(2013)**, pp. 388-393.
[16] C. Muramatsu, T. Nakagawa, A. Sawada, Y. Hatanaka, T. Hara, T. Yamamoto and H. Fujita, "Automated segmentation of optic disc region on retinal fundus photographs: Comparison of contour modeling and pixel classification methods", Computer methods and programs in biomedicine, vol. 101, **(2011)**, pp. 23-32.
[17] E. J. Carmona, M. Rincon, J. G. Feijoo and J. M. Martinez-de-la-Casa, "Identification of the optic nerve head with genetic algorithms", Artificial Intelligence in Medicine, vol. 43, **(2008)**, pp. 243-259.
[18] R. Gonzalez, R. Woods and S. Eddins, "Digital image processing using MATLAB", Pearson Education.
[19] C. Li, C. Xu, *C. G*ui and M. D. Fox, "Distance Regularized Level Set Evolution and its application to Image Segmentation", IEEE transactions on image processing, vol. 19, **(2010)**, pp. 3243-3254.
[20] M. Petrou and P. Bosdogianni, "Image Processing: the fundamentals", West Sussex, John Wiley and Sons, **(2001)**.
[21] J. Kennedy, R. Eberhat and Y. Shi, "Swarm Intelligence", San Fransisco, Morgan Kaufmann publishers, **(2001)**.
[22] D. F. Specht, "A General Regression Neural Network", IEEE transactions on neural network, vol. 2, **(1991)**, pp. 568-576.
[23] J. Canny, "A computational approach to edge detection", IEEE Trans. on pattern analysis and machine intelligence, vol. 8, **(1986)**, pp. 679-698.
[24] Y. Xu, Y. Liu, F. Yin, N. M. Tan, D. W. K. Wong, M. Baskaran, C. Y. Cheng and T. Y. Wong, "Efficient optic cup localization using regional propagation based on retinal structure priors", Proceedings of 34th international Conference of IEEE EMBS, San Diego, California, **(2012)**, pp. 1430-1433.
[25] K. Lewenstein, "Radial basis function neural network approach for the diagnosis of coronary artery disease based on the standard electrocardiogram exercise test", Medical & Biological Engineering & Computing, vol. 39, **(2001)**, pp. 1-6.
[26] T. Teng, M. Lefley and D. Claremont, "Progress towards automated diabetic ocular screening: A review of image analysis and intelligent systems for diabetic retinopathy", Medical and Biological Engineering and Computing, vol. 40, **(2002)**, pp. 2-13.
[27] M. H. A. Fadzil, L. I. Izhar, H. Nugroho and H. A. Nugroho, "Analysis of retinal fundus images for grading of diabetic retinopathy severity", Medical & Biological Engineering & Computing, vol. 49, **(2011)**, pp. 693–700.

Authors

Medha V. Wyawahare, has received degrees, B.E (Electronics) and M. Tech (Electronics) from Nagpur University, Maharashtra State, India in 1993 and 2003 respectively. She is presently working as Assistant Professor in the Department of Electronics, Vishwakarma Institute of Technology, Pune Maharashtra State, India. She is a member of professional bodies like Indian society of technical Education and Institution of Engineers. Her research

interests include Medical Image processing and soft computing techniques.

Pradeep M. Patil, received his B. E. (Electronics) degree in 1988 from Amravati University, Amravati, (India) and M. E. (Electronics) degree in 1992 from Marathwada University, Aurangabad, (India). He received Ph.D. degree in Electronics and Computer Engineering in 2004 from Swami Ramanand Teerth Marathwada University, (India). He is presently working as Director at RMD Sinhagad Technical Institutes Campus, Warje, Pune, Maharashtra state, India. He is member of various professional bodies like IE, ISTE, IEEE and Fellow of IETE. He has been recognized as a PhD guide by various Indian universities. His research areas include pattern recognition, neural networks, fuzzy neural networks and power electronics. His work has been published in various reputed international and national journals and conferences including IEEE and Elsevier.

